Anisotropic effects of non-axial seismic wave propagation in foliated crustal rocks

David A. Okaya
Department Earth Sciences, University of Southern California, USA

Nikolas I. Christensen
Department Geology and Geophysics, University of Wisconsin-Madison, USA

Received 26 October 2001; revised 3 February 2002; accepted 19 February 2002; published 4 June 2002.

[1] Seismic wave propagation within the crust is usually in directions not parallel to inherent rock symmetry axes due to geologic dips of structures and/or oblique-to-arcuate raypaths. We use Christoffel equations and petrophysically measured velocities of crustal metamorphic rocks to examine anisotropic velocities and traveltime effects as functions of non-axial propagation. P- and S-wave velocities are trigonometrically weighted between fast and slow axial velocities. Averaging over a range of non-axial angles yields effective velocities as encountered by through-going crustal raypaths. Axial velocities cannot be simply used to quantify crustal anisotropic effects. The angular behavior of P-wave delay and shear wave splitting are sensitive to V_P measured diagonal to the material symmetry axes; this diagonal velocity controls the presence or absence of non-axial shear wave singularities. These behavior help quantify the contributions of crustal rocks to observations of seismic anisotropy which can serve as proxies for crustal deformation. *INDEX TERMS:* 7203 Seismology: Body wave propagation; 7260 Seismology: Theory and modeling; 7205 Seismology: Continental crust (1242); 5102 Physical Properties of Rocks: Acoustic properties

Author's Personal Copy

1. Introduction

[2] Geological causes of crustal anisotropy include aligned regional fractures and cracks, isotropic heterogeneity or layering, and lattice preferred orientations of highly anisotropic minerals. The presence of shear or metamorphic foliations in fault zones and metamorphic terranes can serve as proxies for intracrustal deformation in a manner analogous to lattice preferred orientation of olivine produced by mantle shear [e.g., *Silver and Chan*, 1991; *Savage*, 1999]. As a result, mapping the lateral and vertical extent of terranes possessing anisotropic behavior ("anisotropic terranes") may define the breadth and magnitude of tectonic processes.

[3] Critical to the production of crustal anisotropy is the relative angle between the seismic wave propagation direction and the foliation of crustal material even as either change along the propagation raypath (Figure 1) Seismic waves propagating within the crust include near-vertical teleseismic waves, depth-to-surface regional or local seismicity waves, and those from surface active sources which have possible "double-effect" downward and upward paths. The paths of these seismic waves may be arcuate or turning due to the presence of velocity gradients within the crust. While major deformational features exist which have internal structure which are oriented horizontal (e.g., the ductile crust of the Basin and Range [*Allmendinger et al.*, 1987]) or vertical (the strike-slip fault system of the San Andreas fault [*Hill et al.*, 1990]), elsewhere the crust internally can be heterogeneous with structures that have broad ranges of orientations. Seismic propagation not parallel or perpendicular to anisotropy axes is more likely the norm within the crust and careful attention must be paid to the anisotropic behavior for non-axial propagation directions at angles intermediate to the anisotropic symmetry axes and the foliation planes.

2. Non-Axial Propagation Velocities for Crustal Rocks of Hexagonal Symmetry

[4] P- and S-wave behavior in non-axial directions of propagation can be better understood with the aid of Christoffel equations [*Christoffel*, 1877]. These equations can be used to obtain P- and S-wave velocities at a relative propagation angle, γ, inclined to material symmetry axes (Figure 1) provided axial and diagonal velocities are known or measured. For hexagonal symmetries these equations reduce to [*Musgrave*, 1970]:

$$\begin{aligned} qV_P^2(\gamma) &= (1/2\rho)\left[c_{11}\sin^2\gamma + c_{33}\cos^2\gamma + c_{44} + M^{1/2}\right] \\ qV_{SV}^2(\gamma) &= (1/2\rho)\left[c_{11}\sin^2\gamma + c_{33}\cos^2\gamma + c_{44} - M^{1/2}\right] \qquad (1) \\ qV_{SH}^2(\gamma) &= (1/\rho)\left[c_{66}\sin^2\gamma + c_{44}\cos^2\gamma\right] \end{aligned}$$

where $M = [(c_{11} - c_{44})\sin^2\gamma - (c_{33} - c_{44})\cos^2\gamma]^2 + (c_{13} + c_{44})^2 \sin^2 2\gamma$ and the elastic constants are derived from four axial and one diagonal petrophysical measurements (Table 1):

$$\begin{aligned} &c_{11} = \rho V_{P90^\circ}{}^2,\ c_{33} = \rho V_{P0^\circ}{}^2,\ c_{66} = \rho V_{SH90^\circ}{}^2 = [c_{11} - c_{12}]/2, \\ &c_{44} = \rho V_{SV0^\circ}{}^2\ \left(\text{or } \rho V_{SH0^\circ}{}^2 \text{ or } \rho V_{SV90^\circ}^2\right),\ c_{12} = c_{11} - 2\rho V_{SH90^\circ}^2, \\ &c_{13} = -c_{44} + \left[\left(4\rho^2 V_{P45^\circ}^4\right) - \left(2\rho V_{P45^\circ}^2\right)(c_{11} + c_{33} + 2c_{44}) \right. \\ &\qquad \left. + (c_{11} + c_{44}) \times (c_{33} + c_{44})\right]^{1/2}. \qquad (2) \end{aligned}$$

[5] An example of a strongly foliated crustal anisotropic terrane is the Haast schist of South Island, New Zealand [e.g., *Okaya et al.*, 1995; *Godfrey et al.*, 2000]. Laboratory velocity measurements indicate this schist is hexagonal in symmetry. Petrophysically measured principal velocities at 600 MPa (Table 1) may be inserted into the above equations in order to obtain non-axial qV_P, qV_{SV}, and qV_{SH} velocities between 0° and 90° as measured from the schist's hexagonal symmetry axis (Figure 2a). The resulting P-wave velocity is not linear but varies trigonometrically between 0° and 90° and is uniformly slow between 0–40°. The SH-wave, whose pure mode has both propagation and vibration directions in the plane of foliation, has velocity behavior with similar angular variation. The SV-wave, whose pure mode has either propagation or vibration normal to the foliation, reaches a local maximum at approximately 40° before decreasing to its original axial value at

Copyright 2002 by the American Geophysical Union.
0094-8276/02/2001GL014285$05.00

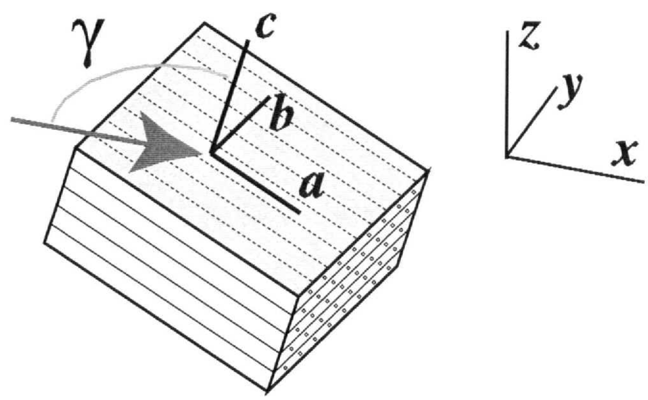

Figure 1. Foliated rock with foliation (planes) and lineation (dashed lines and circles in cross-section) tilted with respect to geographical axes x-y-z. For a hexagonal symmetry approximation, the symmetry axis, c, is normal to foliation while velocities are the same in all directions within the a-b plane. Arrow represents direction of a propagating seismic wave inclined at relative angle γ to the (tilted) symmetry axis.

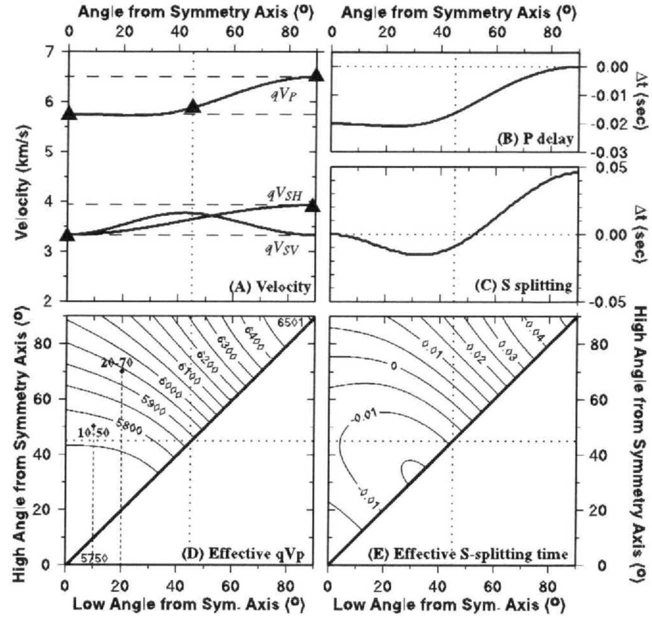

Figure 2. Anisotropic velocity behavior for the Haast schist. (a) Velocities as a function of propagation angle γ relative to hexagonal symmetry axis. qV_P, qV_{SV}, and qV_{SH} velocities are shown for $\gamma = 0-90°$. The five petrophysically measured values are overlain (triangles). For this schist, a qV_{SV}-qV_{SH} crossover exists at 50°. (b) P-wave traveltime delay (sec) per km of propagation with respect to the fastest P at 90°. (c) Amount of shear wave splitting (sec) per km of propagation created by the qV_{SV} and qV_{SH} angular behavior. At 50° the SV and SH switch as to being the earlier-arriving phase. (d) Effective qV_P (m/sec) for a range of propagation angles or geological dips calculated by averaging curves in (a) over a linear distribution of angles. For a given range of dips, e.g., 10–50°, the lower dip is identified on the horizontal axis and the resulting effective velocity can be obtained at height of the higher dip (vertical axis). The effective velocities are in general low and reflect the low qV_P velocities as seen in Figure 2a. (e) Effective shear wave splitting (sec) times per propagation km. Maximum splitting of 0.05 sec per propagation km is obtained for a narrow range of angles (70–90°). At intermediate angles the splitting is neutralized since at low angles the SV and SH velocities are similar.

90°. The SV-wave exhibits 4γ angular variation while the P- and SH-waves exhibits 2γ variation.

[6] Traveltime effects in non-axial directions are shown in Figures 2b–c for the Haast schist. A P-delay is up to 0.02 sec per propagation km for angles within 40° relative to the fast direction at 90°. Shear wave splitting is maximized at 90° where SH is faster than the SV wave. However, the SV wave exhibits "crossover" behavior in that between 0–50° the SV wave is faster, and at 50° a singularity ("crossover point") exists where both S waves have the same velocity with no splitting (Figure 2a). Due to the geometry of hexagonal symmetry, in three dimensions the singularity is conical.

[7] For waves traveling in the crust, a single angle of propagation, γ, is not common. Rather, a range of angles relative to material symmetry axes may be encountered due to directional changes in either raypath dip and/or geological structure. With the use of equations (1) and (2), an effective P-wave velocity can be calculated by averaging over the range of angles which may be encountered upon propagation. Figure 2d illustrates effective P-wave velocities for all possible linear distributions of dips for the Haast schist. For example, a seismic wave encountering a foliated terrane whose dips range uniformally between 10–50° will travel at an averaged, effective P-velocity of 5790 m/s, whereas if the dips ranged from 20–70° the effective velocity is 5945 m/s (Figure 2d). Approximately half of all possible dip ranges result in slow effective velocities (<6000 m/s); only one-third of all dip ranges have an effective velocity greater than the average velocity of the axial P-wave velocities, $(V_{P0°} + V_{P90°})/2$ or 6125 m/s. The broad set of low effective velocities is due to the uniformally low P-wave velocities within 0–50° (Figure 2a). A seismic wave will

Author's Personal Copy

Table 1. Petrophysical velocity measurements of representative foliated crustal rocks. Measurements at 600 MPa.

Rock Type (Locality)	$V_{P0°}$[a] m/s	$V_{P90°}$ m/s	$V_{P45°}$ m/s	$V_{SV0°}$ m/s	$V_{SH90°}$ m/s	density kg/m^3	%Anisotropy[b] VP	VS	ratio	v_{P45}[c]	Refs.[d]
Haast Schist (South Island, New Zealand)	5750	6501	5881	3332	3931	2718	12.3	16.5	1.35	17.4	A,B
Chugach phyllite (Chugach terrane, Alaska)	5994	6547	6084	3456	3931	2723	8.8	12.9	1.46	16.3	C,B
Poultney slate (Vermont, USA)	5403	6639	5826	2781	4059	2781	20.5	37.4	1.82	34.2	D,B
Coldfoot schist (Brooks Range, Alaska)	5800	6357	6059	3294	3948	2657	9.2	18.1	1.97	46.5	E,B
Nanga Parbat Gneiss (N.P., Pakistan)	5856	6331	6230	3351	3685	2656	7.8	9.5	1.22	78.7	F

[a] $V_{P0°}$ = normal to foliation (slower P-wave). $V_{P90°}$ = within planes of foliation (faster P-wave). $V_{P45°}$ = at 45° angle between normal and planes of foliation (intermediate value of V_P). $V_{SV0°} = V_{SV90°} = V_{SH0°}$ = either propagation or particle motion is normal to foliation (slower S-wave). $V_{SH90°}$ = propagation and particle motion both in the foliation planes (fastest S-wave).

[b] %Anisotropy = 100% × $(V_{max} - V_{min})/\{.5(V_{max} + V_{min})\}$ for both P and S velocities. Ratio is VS%-to-VP%.

[c] Normalized V_{P45}° is v_{P45} = 100% × $(V_{P45°} - V_{P0°})/(V_{P90°} - V_{P0°})$ such that v_{P45} ranges between 0–100%.

[d] References: A = *Okaya et al.* [1995]. B = *Godfrey et al.* [2000]. C = *Brocher et al.* [1989]. D = *Christensen* [1965; 1966]. E = *Fuis et al.* [1997]. F = *Meltzer and Christensen* [2001]. Descriptions of mineral assemblages provided in these references.

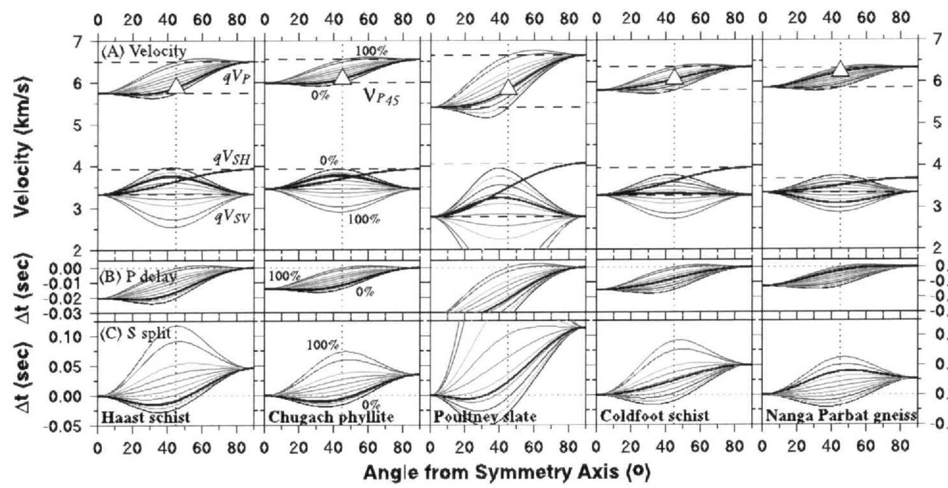

Figure 3. Non-axial velocity behavior for five representative crustal foliated rocks. (a) For each rock, calculated velocities are shown as a function of propagation angle γ relative to hexagonal symmetry axis. qV_P, qV_{SV}, and qV_{SH} velocities are shown (bold lines) for angles of 0–90°. At 90° qV_{SH} is always greater than qV_{SV}. Original velocity measurements at 600 MPa used in calculations are shown as dashed lines (four axial) and open triangle (V_{P45°). (b) Traveltime P-delay per km of propagation for each rock (bold lines). (c) Amount of shear wave splitting per km of propagation (bold lines). In a–c the series of color lines are hypothetical curves of qV_P, qV_{SV}, P-delay, and splitting as functions of hypothetical V_{P45° different from actual V_{P45° (open triangles in Figure 3a). Cold to warm colors denote $\boldsymbol{\nu}_{P45}$ from 0 to 100% every 10%. The magnitude of $\boldsymbol{\nu}_{P45}$ (e.g., Table 1) determines the crossover and singularity behavior of qV_{SV}.

Author's Personal Copy

encounter the fastest P-wave velocities only if propagating at 70–90° from the symmetry axis (within 20° of propagation to the foliation planes). Similar calculations may be made for geologically more-plausible (non-linear or weighted) ranges of dips.

[8] Due to the crossover behavior in the velocities of the SV- and SH-waves, a uniform value of shear-wave splitting is not common. Effective shear-wave splitting times for linear ranges of propagation angles are calculated for the Haast schist (Figure 2e). Maximum splitting is maintained at high propagation angles (70–90°). At moderate angles splitting is negated by the SV-SH crossover. At low angles SV is the earlier-arriving phase but the splitting amounts are small (<0.015 sec per propagation km). There is no splitting for propagation parallel to the symmetry axis. Figures 2d and 2e both indicate that for most directions of propagation the slower Haast velocities are encountered; observations of fast Haast velocities indicate propagation in the narrow range of 70–90° from the symmetry axis.

3. Non-Axial Propagation Velocities for Representative Foliated Crustal Rocks

[9] We next compare our results for the Haast schist with a suite of representative crustal foliated rocks for which petrophysical velocity measurements have been obtained. This suite includes the Chugach phyllite, Alaska, [*Brocher et al.*, 1989]; Poultney slate, Vermont, [*Christensen*, 1965, 1966]; Coldfoot schist, Brooks Range, Alaska [*Fuis et al.*, 1997]; and Nanga Parbat gneiss, Nanga Parbat, Pakistan [*Meltzer and Christensen*, 2001]. Laboratory measured velocities at 600 MPa (equivalent to a crustal depth of ~20 km) for hexagonal symmetry are listed in Table 1. As with the Haast schist, these measurements are inserted into equations (1) and (2) to produce non-axial velocity curves. Figure 3a illustrates the behavior of qV_P, qV_{SV}, and qV_{SH} for these samples. In all cases, qV_P and qV_{SH} vary not linearly but trigonometrically between their slow and fast velocities at 0 and 90°, respectively. qV_{SV} exhibits differing behavior. The Haast schist and Chugach phyllite exhibit S-wave crossover behavior and have faster qV_{SV} at 0 to ~50°. The Poultney slate qV_{SV} nearly equals qV_{SH} between 0–35° (e.g., little S-splitting), above which qV_{SH} becomes the fast S. For the Coldfoot schist and Nanga Parbat gneiss, qV_{SV} is always slower than qV_{SH}, and in the case of the gneiss it is slowest not at 0° or 90° but at 50°. The shear-wave splitting traveltime effects in Figure 3C reflect these relative behavior of qV_{SV} and qV_{SH}. The Poultney slate exhibits a maximum of 0.125 sec splitting per propagation km while the phyllites, schists, and gneiss exhibit .025–0.050 sec per propagation km.

[10] A traditional calculation of anisotropy percentage as defined by *Birch* [1960] is %Anisotropy = $(V_{max} - V_{min})/V_{ave}$ where $V_{ave} = (V_{max} + V_{min})/2$. Calculations of %Anisotropy for P and S velocities for all samples are presented in Table 1. These values show that the ratio of V_S%-to-V_P% anisotropy is not uniform but ranges between 1.22 to 1.97 (Table 1). We attribute this to compositional differences in the anisotropic mineral constituents and is thus rock sample specific; one cannot apply a generalized ratio to obtain the percent anisotropy of a P- or S-wave even if the other wave's percentage is known. We also note that this %Anisotropy calculation uses velocities measured in axial directions, but loses meaning in non-axial directions, particularly with SV and SH waves exhibiting different angular behavior.

4. SV Velocity Behavior and the Role of V_{P45°

[11] As can be seen in Figure 3, the qV_{SV}-qV_{SH} crossover behavior does not necessarily vary according to metamorphic grade. Examination of equations (1) and (2) reveal that qV_P and qV_{SV} have similar derivation and are both sensitive to not only stiffness elements defined by axial velocities, but also to the element c_{13} which itself is sensitive to the diagonal velocity V_{P45°. In order to determine the effects onto the qV_P and qV_{SV} velocities, we calculate for the representative rock samples hypothetical velocity curves using the principal axial velocity measurements (Table 1) and different values of the diagonal velocity based on the normalization formula $\boldsymbol{\nu}_{P45} = (hV_{P45^\circ} - V_{P0^\circ})/(V_{P90^\circ} - V_{P0^\circ}) \times 100\%$ where $\boldsymbol{\nu}_{P45}$ is a percentage between 0 and 100% so that hypothetical diagonal velocity, hV_{P45°, ranges between V_{P0° and V_{P90°.

[12] For the Haast schist in Figure 3a, we compute a series of hypothetical qV_P and qV_{SV} velocity curves where hV_{P45° varies every 10% between the slow and fast axial V_P (cold to warm color curves in Figure 3). At $\boldsymbol{\nu}_{P45} = 0\%$, $hV_{P45^\circ} = V_{P0^\circ}$ and for angles of 20–50° qV_P is actually slower than V_{P0°. Similarly, at $\boldsymbol{\nu}_{P45} = 100\%$, $hV_{P45^\circ} = V_{P90^\circ}$ and qV_P is faster than V_{P90° above 45°. At $\boldsymbol{\nu}_{P45} = 50\%$, hV_{P45° is the average of the two axial P-velocities but qV_P

does not vary linearly between the two axial velocities. Travel time P-delays mimic the hypothetical qV_P curves (color curves in Figure 3b).

[13] qV_{SV} curves also exhibit sensitivity to normalized $\boldsymbol{v}_{P45}$. At $\boldsymbol{v}_{P45}$ = 0%, qV_{SV} reaches a maximum at 40° before returning to $V_{SV0°} = V_{SV90°}$. For the Haast schist, this maximum is slightly larger than the largest SH velocity at $V_{SH90°}$. At $\boldsymbol{v}_{P45}$ = 50%, qV_{SV} is essentially constant with no angular variation. At $\boldsymbol{v}_{P45}$ = 100%, qV_{SV} reaches a large velocity low at 40°. These large magnitude variations in qV_{SV} velocities when compared to qV_{SH} produce a large degree of shear wave splitting over a broad range of angles and $V_{P45°}$ percentages (color curves in Figure 3c). The actual Haast schist sample has a measured $V_{P45°}$ which is at 17.4% above $V_{P0°}$ (Table 1), producing the qV_P and qV_{SV} (bold) curves in Figure 3a and the (bold) S-splitting curve in Figure 3c.

[14] The five representative samples in Figure 3a are arranged in essentially increasing $\boldsymbol{v}_{P45}$; examination of the hypothetical velocity curves in relation to the actual rock sample velocities (Table 1) reveals conditions for qV_{SV} crossover behavior. The Haast schist and Chugach phyllite have low $\boldsymbol{v}_{P45}$ (17.4% and 16.3%, respectively) and a qV_{SV} which exhibits crossover behavior. The Poultney slate at $\boldsymbol{v}_{P45}$ = 34.2% has a qV_{SV} which is nearly the same as qV_{SH} between 0–40° with minor crossover effects and minimal S-spitting. The Coldfoot schist at $\boldsymbol{v}_{P45}$ = 46.5% has a qV_{SV} which is nearly constant and at all angles is slower than qV_{SH}. The Nanga Parbat gneiss at $\boldsymbol{\nu}_{P45}$ = 78.7% has a qV_{SV} with decreased velocity in off-axial directions. In this latter case, the shear wave splitting is maximized not at 90° but at 50° and has a large contribution over a wide range (30–90°) of propagation angles.

5. Discussion and Summary

[15] The magnitudes of fast and slow P- and S-velocities for each foliated crustal rock are unique and are related to mineral assemblages which are controlled by metamorphic grade and rock chemistry. $V_{P45°}$ controls the non-axial behavior of qV_P and qV_{SV} between 0–90° and thus the existence of non-axial propagation shear wave singularities. Failure to detect shear wave splitting in anisotropic crustal sections does not necessarily imply propagation parallel to a hexagonal symmetry axis (e.g., vertical waves through a horizontal foliation). $V_{P45°}$ is not necessarily the simple average of the P-velocities measured at 0° and 90°, thus an accurate assessment of this diagonal P-wave velocity is essential. A more comprehensive database of petrophysical measurements including the diagonal velocities is needed in order to identify a relationship between $\boldsymbol{\nu}_{P45}$, mineral constituents and orientations, and metamorphic grades.

[16] While we have illustrated these angular effects using a hexagonal symmetry approximation, many foliated crustal rocks are more realistically orthorhombic [e.g., *Christensen*, 1965]. In such cases, the three axial planes (*a-b*, *a-c*, *b-c*) have separate angular velocity behavior, requiring three independent $V_{P45°}$ measurements. In addition, the solution for propagation velocities in any non-axial/non-axial plane direction requires the orthorhombic Christoffel equations as functions of both azimuthal and inclination wave directions.

[17] The ability to map the presence and extent of anisotropic terranes is related to the ability of a propagating seismic wave to resolve zones of rock fabrics. Factors which affect this resolution are frequency content and propagation direction of the seismic wavefield with respect to the scale length, continuity, and orientation of the fabrics (terrane breadth and depth plus orientation and continuity of internal structures).

[18] Although complex to analyze, multi-component seismic refraction and reflection experiments may be designed to explicitly seek these terranes using P- or S-wave time delays or polarization or by using perpendicular transects. Polarization and splitting behavior of crustal Ps converted phases which are commonly used in receiver function studies [e.g., *Jones and Phinney*, 1998; *Levin and Park*, 1997] may be used to isolate crustal anisotropy in a manner analogous to mantle SKS shear wave splitting methods. Dense recording arrays used within such experiments may provide sufficient spatial resolution to identify with confidence lateral variations and terminations of an anisotropic terrane. Mantle S- and SKS-splitting results may contain a second-order crustal contribution or alteration to direction and lag if the upcoming seismic waves contain sufficiently high bandwidth to respond to crustal layers.

[19] The need for anisotropic velocity estimation in non-axial directions is critical in crustal wave propagation due to structural heterogeneity (changes in rock orientation) plus changing raypath directions for common crustal seismic waves. Interpretations of crustal seismic data cannot simply use vertical or horizontal orientations of both material symmetry axes and seismic waves unless such orientations exist based on geological and seismic evidence. Such anisotropy when defined through carefully designed field investigations and petrophysical laboratory measurements will provide valuable information on the magnitudes and extent of crustal tectonic deformations.

[20] **Acknowledgments.** We thank Anne Meltzer, Tom McEvilly, Martha Savage, and Nicola Godfrey for discussions regarding the anisotropy of foliated crustal rocks and two anonymous reviewers for their comments. This work was supported by NSF EAR-9418530 and EAR-9980570.

References

Allmendinger, R. W., T. A. Hauge, E. C. Hauser, C. J. Potter, S. L. Klemperer, K. D. Nelson, P. Knuepfer, and J. Oliver, Overview of the COCORP 40°N transect, western United States: The fabric of an orogenic belt, *Bull. Geol. Soc. Amer.*, *98*, 308–319, 1987.
Birch, A. F., The velocity of compressional waves in rocks to 10 kilobars, *J. Geophys. Res.*, *65*, 1083–1102, 1960.
Brocher, T., M. Fisher, E. Geist, and N. Christensen, A high-resolution seismic reflection/refraction study of Chugach-Peninsular terrane boundary, south Alaska, *J. Geophys. Res.*, *94*, 4441–4455, 1989.
Christensen, N., Compressional wave velocities in metamorphic rock at pressures to 10 kilobars, *J. Geophys. Res.*, *71*, 6147–6164, 1965.
Christensen, N., Shear wave velocities in metamorphic rocks at pressures to 10 kilobars, *J. Geophys. Res.*, *70*, 3549–3556, 1966.
Christoffel, E. B., Uber die Fortpflanzung von Stossen durch elastische feste Korper, *Ann. Mater. pura appl.*, *8*, 193–243, 1877.
Fuis, G. S., J. M. Murphy, W. J. Lutter, T. E. Moore, K. J. Bird, and N. I. Christensen, Deep seismic structure and tectonics of northern Alaska: Crustal-scale duplexing with deformation extending into the upper mantle, *J. Geophys. Res.*, *102*, 20,873–20,896, 1997.
Godfrey, N. J., N. I. Christensen, and D. A. Okaya, Anisotropy of schists: Contributions of crustal anisotropy to active-source experiments and shear-wave splitting observations, *J. Geophys. Res.*, *105*, 27,991–28,007, 2000.
Hill, D. P., J. P. Eaton, and L. M. Jones, Seismicity, 1980–1986, in *The San Andreas fault system*, edited by R. E. Wallace, *U. S. Geol. Survey Prof. Paper 1515*, 115–151, 1990.
Jones, C. H., and R. A. Phinney, Seismic structure of the lithosphere from teleseismic converted arrivals observed at small arrays in the southern Sierra Nevada and vicinity, California, *J. Geophys. Res.*, *103*, 10,065–10,090, 1998.
Levin, V., and J. Park, P-SH conversions in a flat-layered medium with anisotropy of arbitrary orientation, *Geophys. J. Int.*, *131*, 253–266, 1997.
Meltzer, A., and N. Christensen, Nanga Parbat crustal anisotropy: Implications for interpretation of crustal velocity and shear-wave splitting, *Geophys. Res. Lett.*, *28*, 2129–2132, 2001.
Musgrave, M., *Crystal Acoustics*, Holden-Day, San Francisco, Calif., 1970.
Okaya, D., N. Christensen, D. Stanley, and T. Stern, Crustal anisotropy in the vicinity of the Alpine Fault, South Island, New Zealand, *New Zealand J. Geol. Geophys.*, *38*, 579–583, 1995.
Savage, M., Seismic anisotropy and mantle deformation: What have we learned from shear wave splitting?, *Rev. Geophys.*, *37*, 65–106, 1999.
Silver, P. G., and W. W. Chan, Shear-wave splitting and continental mantle deformation, *J. Geophys. Res.*, *96*, 16,429–16,454, 1991.

D. A. Okaya, Department Earth Sciences, University of Southern California, Los Angeles, CA 90089-0740, USA. (okaya@usc.edu)
N. I. Christensen, Department Geology and Geophysics, University of Wisconsin-Madison, Madison, WI 53706, USA. (chris@geology.wisc.edu)

Author's Personal Copy